Atmospheric Environment 294 (2023) 119512

Contents lists available at ScienceDirect

Atmospheric Environment

journal homepage: www.elsevier.com/locate/atmosenv

Transboundary haze from peatland fires and local source-derived $PM_{2.5}$ in Southern Thailand

Preyapon Promsiri [a,b], Surajit Tekasakul [c], Thunyapat Thongyen [d], Panwadee Suwattiga [e], John Morris [f], Mohd Talib Latif [g], Perapong Tekasakul [a,h], Racha Dejchanchaiwong [a,i,*]

[a] Air Pollution and Health Effect Research Center, Prince of Songkla University, Hat Yai, Songkhla, 90110, Thailand
[b] Energy Technology Program, Department of Specialized Engineering, Faculty of Engineering, Prince of Songkla University, Songkhla, 90110, Thailand
[c] Department of Chemistry, Faculty of Science, Prince of Songkla University, Hat Yai, Songkhla, 90110, Thailand
[d] Department of Technology and Environmental Management, Faculty of Environment, Kasetsart University, Bangkok, 10900, Thailand
[e] Department of Agro-Industrial, Food and Environmental Technology, Faculty of Applied Science, King Mongkut's University of Technology North Bangkok, Bangkok, 10900, Thailand
[f] School of Industrial Education and Technology, King Mongkut's Institute of Technology Ladkrabang, Bangkok, 10520, Thailand
[g] Department of Earth Sciences and Environment, Faculty of Science and Technology, Universiti Kebangsaan Malaysia, Bangi, 43600, Selangor, Malaysia
[h] Department of Mechanical and Mechatronics Engineering, Faculty of Engineering, Prince of Songkla University, Hat Yai, Songkhla, 90110, Thailand
[i] Department of Chemical Engineering, Faculty of Engineering, Prince of Songkla University, Hat Yai, Songkhla, 90110, Thailand

HIGHLIGHTS

- Influence of peatland fires in Indonesia was as far as southern Thailand.
- High OC/EC in transboundary haze period indicated main source from biomass burning.
- Secondary aerosol was important during transboundary haze period.
- Transboundary haze caused an increase of PAHs and BaP-TEQ concentrations.
- Background $PM_{2.5}$ was mainly from diesel combustion and local biomass burning.

GRAPHICAL ABSTRACT

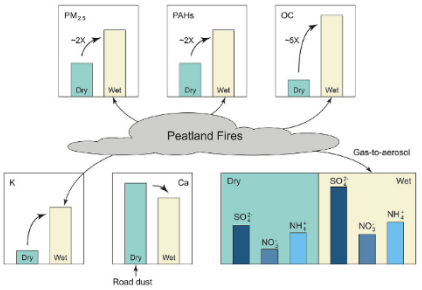

ARTICLE INFO

Keywords:
Fine particles
Transboundary haze
Peatland fires
CMB
ASEAN haze

ABSTRACT

This study characterizes impacts on $PM_{2.5}$ of transboundary haze from peatland fires in Indonesia and local emission sources during 2019–2020 to a large and densely populated city, Hat Yai in southern Thailand. Organic carbon (OC), elemental carbon (EC), water soluble organic carbon (WSOC), water soluble ions (WSI: Cl^-, NO_3^-, SO_4^{2-} and NH_4^+), element tracers (K, Na, Mg and Ca), heavy metals (Cr, Co, Pb, Cd, Ni, Mn) and As, and 16 polycyclic aromatic hydrocarbon (PAHs) components from $PM_{2.5}$ samples (n = 18) were measured to identify local and regional emission sources using a chemical mass balance (CMB) model. We used a combination of air mass backward trajectories and CMB source apportionment to identify $PM_{2.5}$ sources. An increase of $PM_{2.5}$ and chemical component concentrations, during the transboundary haze period, were clearly influenced by aerosols from open biomass burning in Indonesia: PAH concentrations were 2 times higher and OC concentrations, 5 times higher. Secondary organic carbons were predominant during transboundary haze periods, accounting for 52–58% of total OC, indicating higher secondary organic aerosol formation. High K levels demonstrated that the

* Corresponding author. Air Pollution and Health Effect Research Center, Prince of Songkla University, Hat Yai, Songkhla, 90110, Thailand.
E-mail address: racha.d@psu.ac.th (R. Dejchanchaiwong).

https://doi.org/10.1016/j.atmosenv.2022.119512
Received 3 January 2022; Received in revised form 3 October 2022; Accepted 22 November 2022
Available online 29 November 2022

dominant source during this period was biomass burning. Whereas a high level of Ca in the background air came from urban road dust, as well as local biomass burning. Moreover, the increased concentration of SO_4^{2-}, NH_4^+ and NO_3^- during the wet season, as well as transboundary haze periods, was mainly derived the secondary inorganic aerosol formation. Effect on $PM_{2.5}$ concentration from a volcanic eruption near the air mass trajectory during the sampling period was minimal. However, it may have contributed slightly to an increase of SO_4^{2-} concentration in $PM_{2.5}$. Sources of $PM_{2.5}$ in Hat Yai were clearly influenced by local emission sources, e.g. diesel combustion and biomass burning (rubber wood and rice straw), transboundary haze and also secondary organic and inorganic aerosols.

1. Introduction

Transboundary and domestic aerosols caused by burning of biomass resulting from land clearing and resource collection activities, as well as forest fires, have become a serious issue in lower Southeast Asia (SEA) (Tham et al., 2019; Fujii et al., 2019; Sulong et al., 2017; Jaafar et al., 2018; Sulong et al., 2019; Chomanee et al., 2020). Generally, 80–90% of biomass burning emission over a large area contributes highly visible smoke and a high concentration of fine particles to the atmosphere (Adam et al., 2020). The dense haze impacted air quality and climate and led to harmful effects on human health (Ramakreshnan et al., 2017; Apte et al., 2018; Ho et al., 2019; Rajput et al., 2018). Othman et al. (2014) associated the smoke haze to increased inpatient cases by 2.4 per 10,000 people each year, or 31% more than from haze-free days in Malaysia.

Southeast Asia is a fast-growing economic region, where urbanization and industries have increased air pollution especially in big cities. The concentration and chemical composition of atmospheric particles in lower SEA countries was affected by diverse sources, including long-range transport, vehicles, industrial processes, local crop residue open burning and secondary formation of aerosols (Engling et al., 2014; Latif et al., 2018; Chomanee et al., 2020; ChooChuay et al., 2020a; Phairuang et al., 2020). For southern Thailand, rubber wood burning influenced air quality of Hat Yai city during year 2005, based on total suspended particles (Tekasakul et al., 2008). Phairuang et al. (2020) also showed that ultrafine particles ($PM_{0.1}$) came from both vehicle combustion and biomass burning, even when biomass burning dominated. Also, $PM_{2.5}$ in Phuket, Thailand, during 2017–2018, was derived from biomass burning, diesel emissions, sea salt aerosols and industrial emissions as the primary emission sources (ChooChuay et al., 2020a). Forest fires and peat burning in Indonesia was the major domestic source of haze (Betha et al., 2013; Fujii et al., 2014, 2017; Tham et al., 2019), but transboundary pollution affected several neighboring countries: Malaysia (Tahir et al., 2013a, 2013b; Jamhari et al., 2014; Ling et al., 2015; Fujii et al., 2015, 2016a, 2016b; Khan et al., 2016; Sulong et al., 2017, 2019), Singapore (Betha et al., 2014; Engling et al., 2014; Xu et al., 2014; Urbancok et al., 2017; Budisulistiorini et al., 2018; Chen and Taylor, 2018; Tham et al., 2019; Adam et al., 2020) and southern Thailand (Chomanee et al., 2020; Phairuang et al., 2020). In Indonesia, $PM_{2.5}$ emitted from peatland fires in Riau Province, Sumatra, Indonesia during the 2012 haze event was as high as 7120 μg/m^3, or ~300 times as high as the background concentrations (Fujii et al., 2019). Fujii et al. (2019) studied the water-soluble ionic (WSI) components of $PM_{2.5}$ from peatland fires at sources and receptor sites in Riau. High concentrations of Cl^-, $C_2O_4^{2-}$, NO_3^-, SO_4^{2-} and NH_4^+ were observed during the peatland fire-induced haze periods. The increase of WSI concentrations during haze periods can mainly be derived from the gas-to-aerosol conversion. In Malaysia, $PM_{2.5}$ concentrations during the 2013 haze period ranged from 14.5 to 160.9 μg/m^3 (Jaafar et al., 2018). Sulong et al. (2019) reported that polycyclic aromatic hydrocarbon (PAH) concentration, during the 2015 haze period, was 3.40 ± 0.68 ng/m^3, ~2.5 times higher than those during normal periods (1.37 ± 0.09 ng/m^3). Khan et al. (2015) reported that the predominant ions and trace species were NH_4^+, K^+, Ca^{2+}, Na^+, Zn, Al, Mg, and Fe, during the 2014 haze period.

The chemical mass balance (CMB) model and backward trajectory simulations indicated movement of air masses over Sumatra, the largest source of biomass burning in lower SEA, caused the severe haze episodes in southern Thailand (Mahasakpan et al., 2023). Fine and ultrafine particles, during the 2019 haze period in southern Thailand, were dominated by peatland fires accounting for more than 50% of them. Also, Chomanee et al. (2020) reported that PAH concentrations in PM, during the 2015 haze period in southern Thailand, were 2–30 times higher than in the 2017 haze-free period. $PM_{0.1}$ and PAH concentrations during the 2015 haze period were 3.7–23.6 μg/m^3 and 1.1–4.8 ng/m^3, much higher than those during the 2017 normal period (0.4–0.8 μg/m^3 and 0.3–0.4 ng/m^3). The positive matrix factorization (PMF) receptor model and backward trajectory simulations indicated movement of air masses over Sumatra affected severe haze episodes in Malaysia. Fujii et al. (2017) also found a nearly 30% contribution from peatland fires to $PM_{2.5}$ levels in Kuala Lumpur, Malaysia. Fujii et al. (2016b) suggested that a PyC/OC4 ratio >4 implicated biomass burning from Indonesian peatland fires as the haze source. This was consistent with Khan et al. (2015), who reported biomass burning as a haze source, leading to PyC/OC4 > 4, compared to a non-haze period with PyC/OC4 < 2. Jamhari et al. (2014) used principal component analysis (PCA) to identify the sources of organic and inorganic compositions in airborne particulate matters in Malaysia. In Singapore, $PM_{2.5}$ concentrations in 2012–2015 ranged from 87.8 to 317.0 μg/m^3 during the haze period, or ~27 times higher than in a smoke free period (11.5–60.4 μg/m^3). High levels of total carbon (TC), levoglucosan, K^+, SO_4^{2-}, as well as high ratios of organic carbon (OC)/elemental carbon (EC) (14.9 ± 2.9), OC/Levoglucosan (15.3 ± 5.0) and PyC/OC4 (4.8 ± 0.5), indicated that the sources were biomass burning (Tham et al., 2019). They also reported that transboundary haze from peatland fires increased total average OC concentration in $PM_{2.5}$ in Singapore (receptor site) during the strong haze period (92.2 ± 38.7 μg/m^3), up to 20 times higher than in the haze-free period (4.25 ± 1.91 μg/m^3), with OC accounting for up to 94% of TC. This was consistent with large fractions of OC at the source sites (Jambi, Indonesia), with means of 72.6 ± 14.3 μg/m^3 and accounting for an average 95% of total C. Moreover, organic aerosols constituted a significant fraction, 20–60%, of PM, in which WSOC accounted for from 20 to 80% of total OC (Tang et al., 2016; Zhang et al., 2017). The WSOC/OC ratio was used to infer the secondary formation and aging aerosols (Ram et al., 2008, 2012). Also, PAH concentrations on PM_{10} during the 2015 haze period ranged from 1.07 to 5.97 ng/m^3 compared to 0.68–3.07 ng/m^3 during the haze-free (or normal) period (Urbancok et al., 2017).

Data characterizing $PM_{2.5}$ in southern Thailand are limited and only a few have reported comprehensive chemical composition of $PM_{2.5}$ during transboundary haze periods (Chomanee et al., 2020; Phairuang et al., 2020; Choochuay et al., 2020a). Chomanee et al. (2020) reported that PAH concentrations in PM during the 2015 haze period were 2–30 times higher than the 2017 haze-free period. $PM_{0.1}$ and PAH concentrations during the 2015 haze period were 3.7–23.6 μg/m^3 and 4.8–1.1 ng/m^3, much higher than those during the 2017 normal period (0.4–0.8 μg/m^3 and 0.3–0.4 ng/m^3). In the present study, we characterized $PM_{2.5}$ effects on southern Thailand, resulting from both local and regional sources, especially transboundary haze from peatland fires in Indonesia, that occur almost annually, with a focus on OC, EC, WSOC, WSI (Cl^-, NO_3^-, SO_4^{2-} and NH_4^+), element tracers (K, Na, Mg and Ca), heavy metals

(Cr, Co, Pb, Cd, Ni, Mn) and As, and 16 PAHs. Hat Yai City (7.016°N 100.460°E) in Songkhla Province was used as a study site, because it is the largest and most densely populated city in the south of Thailand, where sources of $PM_{2.5}$ are mixed and vary with the season. Furthermore, the sources of ambient aerosols were then identified by source apportionment methods including chemical mass balance (CMB) and OC/EC ratios. Air mass backward trajectory simulation confirmed the PM sources. Also, human exposure risks were estimated from BaP Toxic Equivalence Quotients (BaP-TEQ) of $PM_{2.5}$ bound PAHs.

2. Methodology

2.1. Sampling site

Hat Yai is an urbanized and industrialized city. Close to the ocean, it has a tropical climate with a relatively high and uniform temperature (TMD, 2021). Concentrations of airborne particulate matter and other gaseous pollutants in Hat Yai are not only affected by growing urbanization (traffic volume, commercial and industrial activities), but also transboundary haze, which is most significant during the annual southwest monsoon with air masses passing over Sumatra, Indonesia, as described by Chomanee et al. (2020). Prince of Songkla University (PSU), in the northeast of Hat Yai City (N 7.00511, E 100.50142), was selected as a sampling site to confirm the physical and chemical characteristics of $PM_{2.5}$ affected by the haze, as shown in Fig. S1. The sampling point was ~4 m above ground to study atmospheric air quality with minimum disturbance from local sources (U.S.EPA, 2016).

2.2. Aerosol sample collection

$PM_{2.5}$ samples were collected on a 47-mm quartz fiber filter (2500QAT-UP, Pallflex, USA) using an impactor air sampler with 2.5 μm cut size, developed by Intra et al. (2013), operating at a 5.4 L/min flow rate for approximately 14 days for each sample (n = 18). We took samples every 14 days because we wanted to sample at a flow rate comparable to human breathing rate to observe long-term effects (Thongyen et al., 2015). Average daily $PM_{2.5}$ concentration obtained from the Pollution Control Department (PCD) monitoring station located in the city, ~3 km away from the sampling site (PCD, 2021), during the background period (June–July 2019&October 2019–May 2020), where there were no abrupt changes of sources was 19.5 μg/m^3, with standard deviation 5.6 μg/m^3. In the transboundary haze period (September 2019), the standard deviation was 7.9 μg/m^3 compared to an average $PM_{2.5}$ concentration of 54.2 μg/m^3 (Fig. S2). No samples were taken across changes in the monsoon seasons. Quartz fiber filters were baked at 350 °C for 1 h prior to use (Kumsanlas et al., 2019). Before and after collection, they were stored in a desiccator with controlled relative humidity 50 ± 5% at room temperature for 72 h. The filter was then weighed by a 0.01 mg resolution balance (CP225D, Sartorius, Germany). After the weighing, filter samples were kept in a plastic bag wrapped by aluminium foil and stored at 4 °C to maintain their chemical stability until analysis (Tang et al., 2005; Furuuchi et al., 2007). The samples were collected approximately twice a month, back to back. However, some samples in the months of August and December 2019, and January 2020 were unusable, due to filter tear after sampling: these samples were not included for analysis to avoid possible errors. Others were missed due to technical problems with the equipment. Meteorological parameters, including temperature, relative humidity (RH), rainfall, wind speed (WS) and wind direction (WD) during 2019–2020 were obtained from Thai Meteorological Department, Hat Yai, Songkhla, Thailand (TMD, 2021), as shown in Table S1. The climate in the southern part of Thailand may be divided into two major monsoon seasons: the northeast monsoon from December to March and the southwest monsoon covers May to October (Adam et al., 2020). It can also be divided into two seasons depending on the rainfall: a dry season (January–April) and a wet season (May to December) (Phairuang et al., 2020). In this study, twelve samples during June 2019 to November 2019 and May 2020 represented the “wet season” coinciding largely with the southwest monsoon. Six samples in the remaining months represented the “dry season”, coinciding with the northeast monsoon. Furthermore, we selected the "transboundary haze period” in September 2019 (n = 2), when hotspots in lower SEA were clearly present, resulting in high $PM_{2.5}$ concentrations >40 μg/m^3, measured by the PCD monitoring station as shown in Fig. S2. Two sampling periods in September covered most of the month (3–13 Sep 2021 and 18–25 Sep 2022), when the $PM_{2.5}$ concentration was higher than 40 μg/m^3 as a result of transboundary haze. However, the transboundary haze also partially affected Hat Yai air quality, during June–August 2019, resulting in slightly higher PM concentrations than October 2019 to May 2020. Transboundary haze in this study was formed from particles, usually emitted from open biomass burning over a large area, and transported across borders to neighboring countries (Adam et al., 2020). Contributions of particulate matters observed in Hat Yai city were assigned to either (a) local (diesel engines, industrial biomass, agricultural waste) or (b) regional (transboundary haze from peatland fires in Indonesia) sources. Background air represents year-round ambient levels of pollutants, excluding September.

Air mass backward trajectories (BT) of air and aerosol particles from possible local and regional sources were simulated using the Hybrid Single-Particle Lagrangian Trajectory (HYSPLIT) model (Air Resources Laboratory, 2021). Wind direction at 1000 m altitude (AGL) was selected and the start time for backward trajectories was 00UTC (0700 Bangkok time) to observe long range transport of pollutants. Hotspots from open biomass burning were obtained from the NASA VIIRS 375 m active fire data (Earthdata, 2021). More details of the analytical methods for BT are described by Dejchanchaiwong and Tekasakul (2021).

2.3. Chemical analysis

We analyzed $PM_{2.5}$ for its chemical components, including 16 PAHs, OC, EC, WSOC, WSI (Cl^-, NO_3^-, SO_4^{2-} and NH_4^+), four element tracers (K, Na, Mg and Ca) and six heavy metals (Cr, Co, Pb, Cd, Ni and Mn) and As to apportion $PM_{2.5}$ sources in Hat Yai City by using a CMB model, PAH diagnostics and OC/EC ratios. For samples collected in the first half of each month (sample#1), the quartz fiber filter samples were cut into two halves. The first was used to analyze the PAH components and the other was further cut into two halves for carbonaceous, and WSI, and heavy metal (HM) and As analysis. Filter samples collected in the second half (sample#2) were also cut into halves: one half for PAH analysis and the other was again cut into half for carbonaceous, and WSOC analysis.

For PAH analysis, one half of each filter sample was extracted using an ultrasonic bath (Furuuchi et al., 2007). The extracted solution was filtered through a 0.45 μm PTFE syringe filter and 50 μL of dimethyl sulfoxide was added. The residue was re-dissolved in 450 μL acetonitrile and filtered again. PAHs were analyzed by High-Performance Liquid Chromatography (HPLC, 1100, Agilent, Germany, UPS C-18 column, 5 μm, 4.6-mm diameter, 250-mm length) with coupled diode array and fluorescence detectors (HLPC-DAD/FLD).

Carbon was analyzed using a carbon aerosol analyzer (Model 5, Sunset Laboratory, USA), following the Interagency Monitoring of Protected Visual Environments (IMPROVE) protocol with the Thermal Optical Reflectance (TOR) correction scheme. Four OC fractions (OC1, OC2, OC3 and OC4) and three EC fractions (EC1, EC2, and EC3), and the pyrolyzed OC (PyC) were analyzed. The samples were punched to 1.5 cm^2 using a rectangular cutter. Details of analytical methods for the carbonaceous fractions can be found elsewhere (Dejchanchaiwong et al., 2020; Phairuang et al., 2020). The concentrations of primary organic carbon (POC) and secondary organic carbon (SOC) were investigated following the EC-tracer method based on the minimum OC/EC ratio (Sresawasd et al., 2021).

For elemental tracers and heavy metals and As, a filter was extracted

with 2 mL nitric acid in an ultrasonic bath (95 °C, 1 h) and then 50 μL hydrogen peroxide was added, and continuously extracted in an ultrasonic bath for 30 min. The extracted solution was filtered through the filter and diluted with deionized water. The elemental tracers, heavy metals and As were analyzed using Inductively Coupled Plasma Optical Emission Spectrometer (ICP-OES) (AVIO 500, PerkinElmer, Germany). For WSI components, a filter was extracted with 25 mL pure water (specific resistivity >18.2 MΩ) in an ultrasonic bath for 30 min. The extracted solution was filtered through a 0.45 μm PTFE syringe filter. 20 mL of extracted solution was used to determine Cl^-, NO_3^- and SO_4^{2-} concentrations by an Ion Chromatograph (DX-500, DIONEX, USA) and another 5 mL of extracted solution was analyzed for NH_4^+ using an Ammonium Test-kit and photometric technique (Spectroquant Prove 300, Merck, USA). Details of the WSI analysis are given by Samae et al. (2021).

The filter sample for WSOC analysis was extracted with 20 mL pure water (specific resistivity >18.2 MΩ) in an ultrasonic bath (Ultrasonicator, Elma, Germany) (10 °C, 15 min). The extracted solution was then analyzed using by total organic carbon (TOC) analyzer (multi N/C 3100, Analytik Jena, Germany) to determine WSOC. The limit of detection (LOD) was 0.02 mg/L and for quantification (LOQ) was 0.06 mg/L.

2.4. Quality assurance and quality control

A quality assurance/quality control procedure for each analysis was followed. All field and laboratory blank filters were analyzed. Each sample was kept in a plastic bag wrapped by an aluminium foil before analysis. Chemical component concentrations in the blank filters (n = 3) were subtracted from the samples. Before each carbon analysis, the total carbon (TC) value was calibrated by the reference, sucrose standard (3.206 μg C μL^{-1}) (Sunset Laboratory Inc., USA). The detection limit for both the OC and EC carbon analyzer was 0.2 μg C cm^{-2}. A linear correlation between the sucrose standard solution concentrations and measured concentration was found, $R^2 = 0.995$. Coefficient of variation of the instrument did not exceed 10% for TC to ensure precision. ICP-OES element detection limits, in μg/L, were As – 20, Cd – 1, Co – 1, Cr – 2, Mn – 0.4, Ni - 5, Pb – 10, K - 20, Ca – 0.02, Mg – 0.1 and Na – 3. The WSOC limit of detection (LOD) was 0.02 mg/L and limit of quantification (LOQ) was 0.06 mg/L. Linearity and precision were determined by analysis of dilutions of the 16 PAH reference mixtures (Supelco, Catalog number 4–8743, USA) in acetonitrile, ranging from 0.01 to 20 μg/mL. The recovery of individual PAHs in the spiked samples ranged from 71.0% to 108.4% and detection limits of for individual PAHs ranged from 1.9 to 40.8 ng/mL. A linear correlation between the 16 PAHs-mix reference solution concentrations and peak areas was found, with $R^2 >$ 0.999, for all PAHs, as described in Dejchanchaiwong et al. (2020).

2.5. Source identification

2.5.1. OC/EC ratio

The OC/EC ratios are widely used to identify emission sources. Typical emission sources of OC/EC from the literature include: diesel exhaust (OC/EC: 0.06–0.8) (Dallmann et al., 2014; Na et al., 2004), peatland fire (near source) (OC/EC: 15.0–38.0) (Tham et al., 2019), peatland burning site (OC/EC: 36.4 ± 9.1) (Fujii et al., 2014) and biomass burning (OC/EC: 3.8–13.2) (Zhang et al., 2007).

2.5.2. Chemical mass balance model

The Chemical Mass Balance (CMB) receptor model was also used to identify the emission sources (U.S.EPA, 2005). The CMB model uses the chemical compositions of $PM_{2.5}$ to estimate the source contributions to concentrations at the receptor. We used the CMB8.2 software (U.S.EPA, 2005), obtained from the U.S. EPA website, to identify the sources. The CMB outputs are acceptable when $0.8 \leq R^2 \leq 1.0$, $\chi^2 \leq 4.0$ and percent mass (% mass): 100% ± 20% (U.S.EPA, 2004a). We used the PAH and carbonaceous components dataset, where x_{ij} is the ambient concentration of chemical species (j) measured in sample (i), computed by (U.S. EPA, 2004b):

$$x_{ij} = \sum_{k=1}^{p} g_{ik} f_{kj+} e_{ij} \quad (1)$$

where g_{ik} is the concentration contributed by source (k) to sample (i), f_{kj} is the fractional concentration of chemical species (j) in the emission from source (k) and e_{ij} is the residual concentration of chemical species (j) measured in sample (i).

3. Results

3.1. Air mass backward trajectories

A 72-h BT simulation for Hat Yai, during the transboundary haze period, 18–21 September 2019, is shown in Fig. 1. Simulated air mass trajectories for the southwest wind passing through a high concentration of hotspots, due to peatland fires in south Sumatra, Indonesia carried the transboundary haze towards Hat Yai.

3.2. p.m.$_{2.5}$ mass concentration

Monthly average $PM_{2.5}$ concentrations from two samples in each month during June 2019–May 2020 at the PSU site (in Table 1) varied strongly with the season, from <10 μg/m^3 in the dry season to as high as 32.7 μg/m^3 in the wet season in September (transboundary haze period): a strong correlation with observed hotspots, obtained from ASEAN Specialised Meteorological Center (ASMC, 2021), in Indonesia can be seen in Fig. 2. However, even early in the burning season, transboundary haze in June and July, led to $PM_{2.5}$ levels that were slightly higher than the background (annual average: 8.4 μg/m^3). It is noticeable that in October, although many hotspots were observed, the $PM_{2.5}$ levels dropped as the direction of the monsoon wind changed and little haze was transported to Thailand.

3.3. Distributions of chemical components in $PM_{2.5}$

3.3.1. Carbonaceous components

Concentrations of TC, OC, EC, WSOC, POC and SOC are summarized in Table 1. TC mass concentration in $PM_{2.5}$ during the wet season was typically 5.7 μg/m^3, or twice the ~2.5 μg/m^3 during the dry season, but it reached 15 μg/m^3 during the transboundary haze period (~5 times higher than the background - 2.8 ± 0.5 μg/m^3). Similarly, concentrations for both OC and EC, during the wet season, were ~2.5 and ~1.7 times those during the dry season, and during the transboundary haze period, they were even higher, ~5 and ~3 times higher than background. Even in June and July, OC and EC concentrations were also slightly higher than the background. Contributions of both OC ane EC to $PM_{2.5}$ mass concentration was similar over the year, typically 30% for OC and 9% for EC. However, during transboundary haze periods, OC contributions to $PM_{2.5}$ were usually >50%, but EC was only slightly higher, ~11%, compared to background, OC at ~25% and EC at ~9%. So, the organic carbon fraction was significantly higher in the haze. Water soluble organic concentrations (WSOC) were also ~1.6 times higher in the wet than the dry seasons, but also significantly higher during the transboundary haze period - ~2 times higher at 4.3 ± 1.0 μg/m^3 (42.9 ± 0.2% in OC). The fractional contributions of POC in total OC in the background air was ~76%, while during the transboundary haze period, SOC was dominant, 5.6 ± 1.7 μg/m^3, ~4 times those during the background air (0.5 ± 0.3 μg/m^3). Although the general trends are similar, when we analyze the components in more detail, the following sections show that we can make further inferences, firstly analyzing the order of the dominant components.

Concentrations of eight carbonaceous fractions during the entire

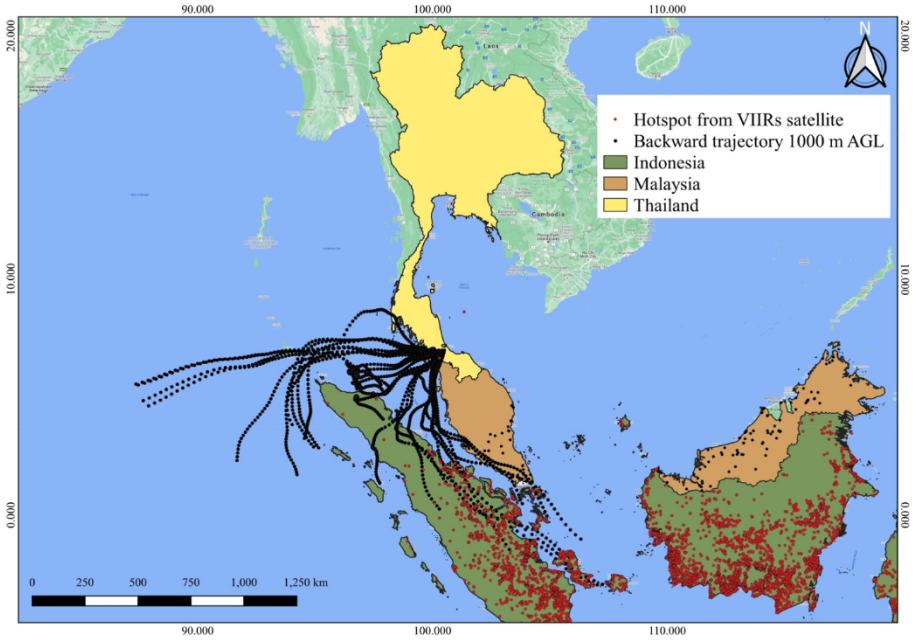

Fig. 1. Backward trajectory simulation for Hat Yai, southern Thailand, during the 2019–2020 haze period on 18–21 September 2019.

Table 1
Monthly average TC, OC, EC, WSOC, POC and SOC mass concentration during wet and dry seasons in Hat Yai city.

Seasons	Periods	Samples	Concentrations (μg/m^3)						
			$PM_{2.5}$	OC	EC	TC	WSOC	POC	SOC
Wet season		Jun 2019	9.5 ± 3.2	2.6 ± 0.4	0.8 ± 0.1	3.4 ± 0.6	0.9	1.7 ± 0.3	0.9 ± 0.1
		Jul 2019	8.0 ± 0.9	2.5 ± 0.2	0.7 ± 0.04	3.3 ± 0.2	0.8	1.5 ± 0.04	1.0 ± 0.2
	Transboundary haze period	Sep 2019#1	13.6	8.3	1.9	10.2	3.6	4.0	4.3
		Sep 2019#2	32.7	11.8	2.4	14.2	5.0	5.0	6.8
		Oct 2019	8.0 ± 2.8	1.9 ± 0.4	0.7 ± 0.2	2.6 ± 0.5	0.5	1.5 ± 0.3	0.4 ± 0.3
		Nov 2019	9.6 ± 3.0	1.8 ± 1.0	0.8 ± 0.5	2.6 ± 1.6	0.7	1.7 ± 1.1	0.1 ± 0.1
		May 2020	10.6 ± 0.1	2.5 ± 0.1	0.9 ± 0.1	3.4 ± 0.1	1.4	1.9 ± 0.1	0.6 ± 0.04
Dry season		Feb 2020	6.0 ± 0.3	1.4 ± 0.2	0.6 ± 0.1	2.1 ± 0.3	0.9	1.3 ± 0.3	0.1 ± 0.1
		Mar 2020	9.6 ± 4.5	2.1 ± 0.5	0.8 ± 0.2	2.8 ± 0.7	0.9	1.6 ± 0.4	0.5 ± 0.1
		Apr 2020	6.1 ± 0.3	2.0 ± 0.7	0.6 ± 0.1	2.6 ± 0.8	1.3	1.3 ± 0.2	0.7 ± 0.4

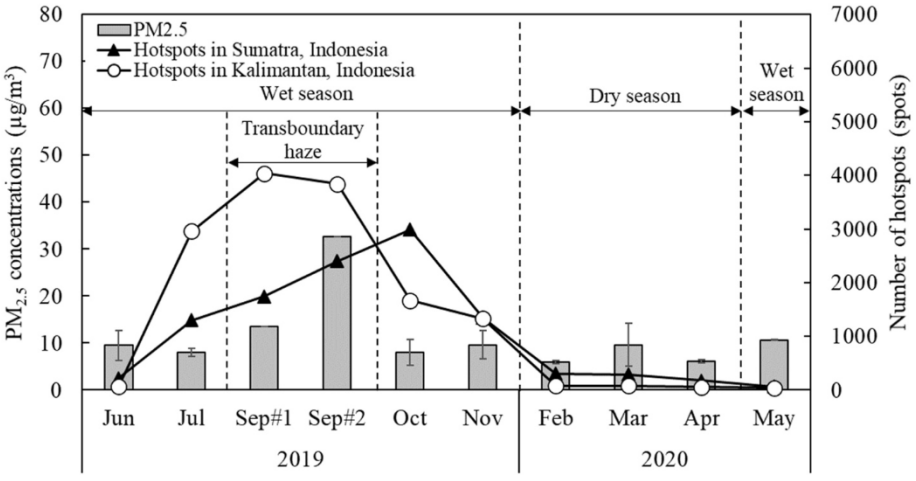

Fig. 2. Monthly $PM_{2.5}$ concentrations (bars) and hotspot counts for June 2019–May 2020 in Sumatra (triangles), and Kalimantan (circles), Indonesia.

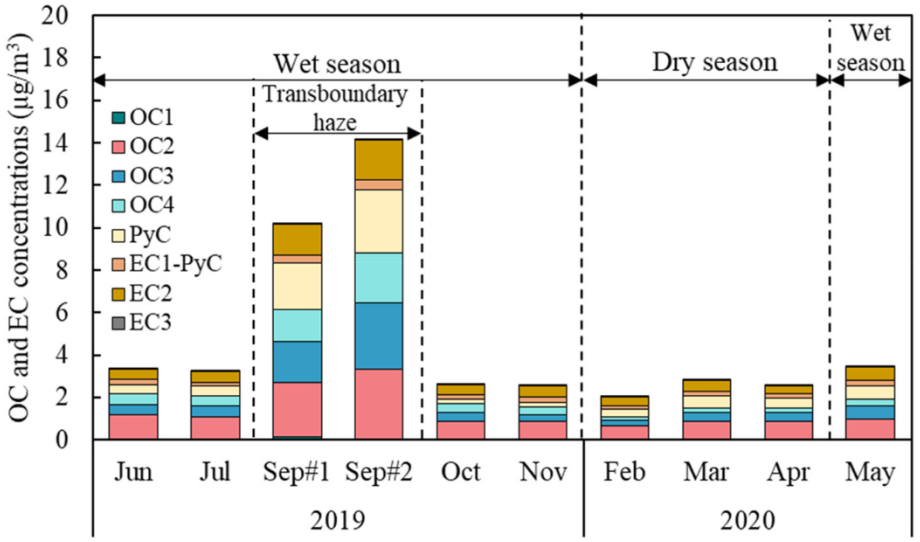

Fig. 3. Distributions of $PM_{2.5}$ carbonaceous components for different periods.

period are shown in Fig. 3. The relative sizes of $PM_{2.5}$ fractions in OC and EC changed slightly with the season and presence of haze:

wet: OC2>OC3>PyC > EC2>OC4>EC1-Pyc > EC3>OC1

dry: OC2>PyC > EC2>OC3>EC1-PyC > OC4>EC3 >OC1

haze period: OC2>OC3>PyC > OC4>EC2>EC1-PyC > OC1>EC3

OC3 and OC2 were the most abundant fractions, during the wet season and the transboundary haze period.

Note that in the following sections, reported numeric values are medians plus inter quartile ranges: the data values are generally significantly skewed, making standard deviations inappropriate.

Table 2
Concentrations of trace elements, heavy metals and As and WSI compositions in $PM_{2.5}$ at the PSU site, Jun 2019–May 2020, covering wet, dry seasons and the transboundary haze period.

Components	Concentration (ng/m^3) –median with interquartile range in parentheses			
	Wet season	Dry season	Transboundary haze	Background air
As	ND	ND	ND	ND
Cd	ND	ND	ND	ND
Co	0.6 (0.3)	ND	0.8	0.5 (0.7)
Cr	2.8 (4.8)	ND	11.4	1.9 (3.3)
Mn	3.2 (3.0)	2.9 (5.7)	5.1	3.0 (3.6)
Ni	0.2 (0.8)	ND	0.4	ND
Pb	ND	ND	3.5	ND
K	438.1 (191.5)	87.5 (49.1)	1153.6	347.8 (280.8)
Ca	792.0 (631.3)	677.5 (362.1)	169.5	792.0 (423.7)
Mg	10.4 (29.1)	141.3 (89.1)	31.9	10.4 (73.3)
Na	8.2 (23.3)	ND	1129.2	ND
NH_4^+	628.1 (330.6)	552.4 (42.0)	944.0	532.5 (142.9)
Cl^-	ND	221.2 (81.3)	ND	191.7 (85.1)
NO_3^-	484.9 (208.8)	244.5 (64.2)	472.0	464.5 (371.5)
SO_4^{2-}	2458.7 (256.3)	1267.4 (223.6)	3421.9	1361.8 (285.2)

Note: Values in this table are medians followed by interquartile ranges in parentheses.
ND – Not Detected.

3.3.2. Distribution of trace elements, heavy metals and As

Table 2 summarizes median and interquartile range (IQR) concentrations of As and heavy metals (Cd, Co, Cr, Mn, Ni and Pb), trace elements (K, Ca, Mg and Na) and WSIs (NH_4^+, Cl^-, NO_3^- and SO_4^{2-}). The highest concentrations of heavy metals in Hat Yai were found in the transboundary haze period, but neither As nor Cd were found in the entire period. However, the concentrations of heavy metals and As in this study were well below National Ambient Air Quality Standards: NAAQS (Pb 0.5 μg/m^3, As 6 ng/m^3, Cd 5 ng/m^3 and Ni 20 ng/m^3 per annual) (EEA, 2008); and Pb 1.5 μg/m^3 per month (PCD, 2021).

Ca and K were the major trace elements during the wet season (typically 1244 ng/m^3), but in the dry season, the total was lower (~819 ng/m^3) and Mg was added to the list of major elements. Ca dominated, contributing 64% in the wet and 83% in the dry season, but the K fraction dropped significantly and was ~5 times lower in the dry season. Mg moved in the opposite direction, bccoming ~14% higher in the dry season. In the haze period, K dominated, accounting for 46% of the much higher totals (~2500 ng/m^3). K is considered as an indicator of biomass burning – coming from plant material, distinct from Ca from dust or degraded rocks in the soil: in our measurements, K was ~3 times higher that the background during haze periods. In background air, Ca from soil minerals dominated (up to 80% of the mass). Na, also from biomass burning, was only observed in significant amounts in the haze period.

3.3.3. WSI distributions

Median and IQR (Interquartile range) of WSI concentrations from $PM_{2.5}$ are also in Table 2. The order of the median total WSI concentrations in $PM_{2.5}$ in the background was: SO_4^{2-} > NH_4^+ > NO_3^- > Cl^-. During transboundary haze period: the order was the same, but no Cl^- was found, SO_4^{2-} was predominant in all periods, with concentrations reaching 3422 ng/m^3 (70.7% of total WSI components), during the transboundary haze period, whereas it$^-$ contributed only 56% during haze-free periods. In the wet season, SO_4^{2-}(Lippmann and Thurston, 1996) and NO_3^- concentrations were approximately double those in the dry season: they are usually associated with high pH, detrimenting health, whereas any increase in NH_4^+ was small (10%).

3.3.4. PAHs and toxicity distribution

PAH concentrations, divided into low molecular weight (LMW-PAHs, 2–3 rings) and high molecular weight (HMW-PAHs, 4–6 rings) groups, and BaP Toxic Equivalence Quotient (BaP-TEQ) concentrations for $PM_{2.5}$ during the wet and dry seasons, and transboundary haze period

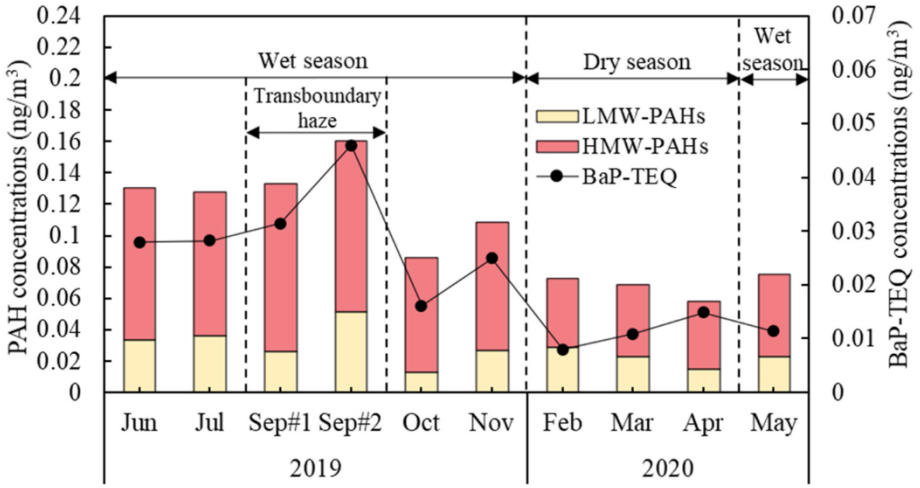

Fig. 4. PAH mass concentrations, for LMW-PAHs and HMW-PAHs, along with BaP-TEQ concentrations for $PM_{2.5}$, during the entire period of this study.

are in Fig. 4. BaP-TEQ is a widely used indicator to evaluate the health risk of PAH exposure (Tekasakul et al., 2008). Total concentrations of 16 PAHs ranged from 0.058 to 0.161 ng/m^3 during the entire sampling period. Overall, PAH concentrations were ~2 times higher in the wet season, where the HMW-PAH fraction was also higher (67.8–84.5%). In the haze period, PAH contributions were also higher: a maximum PAH concentration - 0.16 ng/m^3 - was observed in 18–26 Sep 2019, when the atmosphere in southern Thailand was covered by haze. Average BaP-TEQ concentration for $PM_{2.5}$ during wet season was 0.027 ± 0.011 ng/m^3, ~2 times higher than the dry season - 0.011 ± 0.003 ng/m^3. Similarly, BaP-TEQ concentrations, during the haze period, were ~2 times above the background.

3.3.5. *Potential emission sources of $PM_{2.5}$*

3.3.5.1. Behaviors of OC/EC and WSOC/OC. Carbonaceous aerosols have various sources. The OC/EC ratio is an important index to identify the emission source (Chu, 2005). Typical emission sources of carbonaceous fractions measured by the IMPROVE_TOR method were described by Dejchanchaiwong et al. (2020). Trends in the ratios, OC/EC, EC/TC, OC/TC and WSOC/OC, from Jun 2019 to May 2020, are shown in Table 3. The OC/EC ratio ranged from 2.3 ± 0.3–4.9, with mean 3.4 ± 1.0 during wet season, and 2.30 ± 0.2–3.2 ± 0.5, with mean 2.7 ± 0.5 during dry season. The average OC/EC ratio, during the transboundary haze period, was 4.6 ± 0.4, whereas, in the background air, it was 2.8 ± 0.4. The EC/TC ratio was also widely used as a way to distinguish fossil fuel and biomass burning emissions (Sudheer and Sarin, 2008; Pani et al., 2019): the EC/TC and OC/TC ratios are interpreted in the opposite direction - low EC/TC ratios, 0.1–0.2, indicate biomass burning and higher ratios, whereas ~0.5, indicates fossil fuel combustion (Ram et al., 2008). The average EC/TC and OC/TC ratios during wet seasons were close to 0.2 and 0.8, whereas during dry seasons, they were 0.3 and 0.7. Average EC/TC ratios during transboundary haze period were 0.2 versus 0.3 in the background, whereas OC/TC ratios were 0.8 versus 0.7. The WSOC/OC ratios during wet and dry seasons were 0.4 ± 0.1 versus 0.5 ± 0.1. Similarly, the average WSOC/OC ratios, during the transboundary haze period (0.4), were slightly lower than the background (0.5).

3.3.5.2. CMB model. The major primary source profiles included in the CMB model were: palm fiber, palm kernel, rice straw, rice stubble, rubber wood, diesel (Samae et al., 2021) and peatland fire in Indonesia (See et al., 2007) - provided as input to the model. These are sources that could affect air quality in southern Thailand. Peatland fire samples were collected from Sungai Sembilan (~100 m away from peatland fires) by See et al. (2007). Source contributions of $PM_{2.5}$ during the wet and dry seasons, and transboundary haze period are shown in Fig. 5. The largest contributor during the wet season was peatland fire (45%), followed by diesel (14%), rubber wood (12%), rice straw (8%) and unidentified sources (21%). During the dry season, diesel combustion dominated at 52%, followed by burning rubber wood (18%), rice straw (15%) and unidentified sources (15%). $PM_{2.5}$ sources during the transboundary haze period in Hat Yai were dominated by peatland fire (50%), followed by rubber wood burning (27%), diesel combustion (4%), rice straw (1%) and unidentified sources (18%). Even though secondary aerosol formation was not included in the CMB, it cannot be ignored. It could be a significant portion in other unidentified sources.

Table 3
Seasonal average OC/EC, EC/TC, OC/TC ratios for $PM_{2.5}$ from Jun 2019 to May 2020 in Hat Yai.

Season	Period	samples	Ratios			
			OC/EC	EC/TC	OC/TC	WSOC/OC
Wet season		Jun	3.2 ± 0.1	0.2 ± 0.003	0.8 ± 0.003	0.3
		Jul	3.5 ± 0.2	0.2 ± 0.01	0.8 ± 0.01	0.3
	Transboundary haze period	Sep#1	4.4	0.2	0.8	0.4
		Sep#2	4.9	0.2	0.8	0.4
		Oct	2.7 ± 0.1	0.3 ± 0.01	0.7 ± 0.01	0.3
		Nov	2.3 ± 0.3	0.3 ± 0.02	0.7 ± 0.02	0.6
		May	2.8 ± 0.1	0.3 ± 0.01	0.7 ± 0.01	0.6
Dry season		Feb	2.3 ± 0.2	0.3 ± 0.02	0.7 ± 0.02	0.6
		Mar	2.7 ± 0.03	0.3 ± 0.002	0.7 ± 0.002	0.5
		Apr	3.2 ± 0.5	0.2 ± 0.03	0.8 ± 0.03	0.5

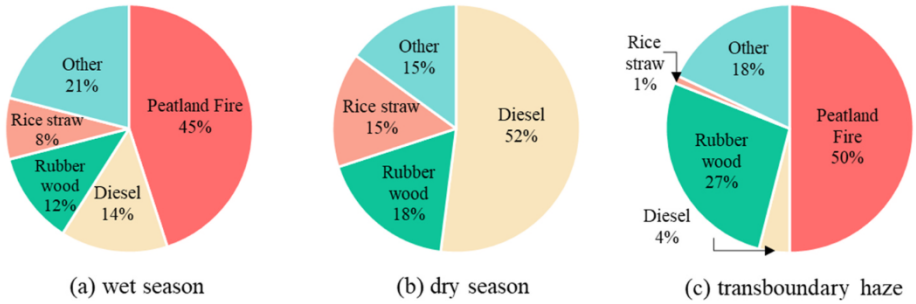

Fig. 5. Source contributions of $PM_{2.5}$ at Hat Yai City.

4. Discussion

Sources of $PM_{2.5}$ in Hat Yai can be determined from chemical components (OC, EC, WSOC WSI, heavy metals and As), source apportionment (OC/EC ratio and CMB model) and the air mass backward trajectory for regional sources. In general, the southwest monsoon prevailed in the wet season, whereas the dry season was dominated by the northeast monsoon. High rainfall and less stagnant air, as well as less open burning, in the wet season contributed to low PM levels, compared to the dry season in many areas in Thailand (Sresawasd et al., 2021). However, this was not the case in southern Thailand, especially during the El Niño years. The $PM_{2.5}$ concentration in Hat Yai, during the 2019 wet season, was approximately 2 times higher than during the dry season. The increase of PM level during the wet season was an regional effect, as no significant change of local sources occurred. Background concentration in the area has been low (annual average: 8.4 $\mu g/m^3$) as a result of local open burning in paddy fields, combustion of rubber wood in local industries, and other sources, including popular diesel pick-up trucks and possibly biogenic and anthropogenic secondary aerosol formation. Peatland fires in Sumatra occur almost annually with varying intensities. Several studies reported that lower SEA air quality, including southern Thailand, was directly influenced by transboundary aerosol transport from Indonesian peatland fires (Sulong et al., 2017, 2019; Jaafar et al., 2018; Latif et al., 2018; Tham et al., 2019; Fujii et al., 2019; Chomanee et al., 2020). This phenomenon was our focus in the beginning of the discussion of the results. Uncontrolled biomass burning was particularly intense in Indonesia, during El Niño years, contributing to air pollution in neighboring countries (Sulong et al., 2017; Samsuddin et al., 2018). During 2019, the number of hotspots from peatland fires was extremely high, because the El Niño-Southern Oscillation (ENSO) enhanced the severity of the situation (Adam et al., 2020). The hotspots in Indonesia rose from June to November mostly in Sumatra and Kalimantan, affecting Hat Yai air quality. The highest $PM_{2.5}$ concentrations were observed during the transboundary haze period (Sep 2019) and were approximately 4 times higher than the background. This agreed with the previous report from the ASEAN Specialised Meteorological Center, showing a high risk of severe transboundary haze on 5, 9 and 29 September 2019 (ASMC, 2021). The backward trajectory simulations also indicated that aerosol transported from open biomass burning area in some parts of Sumatra affected Hat Yai air quality, due to prevailing southwest winds during the transboundary haze periods. This agrees with previous studies showing significant enhancements in $PM_{2.5}$ concentrations. over lower SEA. during the southwest wind period, from 2009 to 2015, e.g. Singapore (Betha et al., 2014; Budisulistiorini et al., 2018), Malaysia (Fujii et al., 2016a) and Indonesia (Uda et al., 2019), with daily $PM_{2.5}$ levels, exceeding local background levels and the WHO guidelines - 25 $\mu g/m^3$. Similarly, increases of $PM_{2.5}$ levels were observed in Thailand (Chomanee et al., 2020). The transport of pollutants especially particulate matter is strongly influenced by a carrying wind. Once the PM is transported to a particular area, meteorological conditions, e.g. temperature, relative humidity and wind in combination, determine how long the pollution persists. In this study, the correlations between $PM_{2.5}$ mass concentrations and precipitation, relative humidity, temperature, and wind speed were not strong through the entire period. However, high wind speed and precipitation favored the dispersion of atmospheric pollutants and reduced PM concentrations, while low wind speed and low precipitation helped pollution levels to rise. (Ouyang et al., 2015). Moreover, the key factors for pollutant residence time are temperature inversions, planetary boundary layer and ventilation rate (Feng et al., 2020).

Carbonaceous aerosols are a significant component of fine particles. The average OC and EC concentration in $PM_{2.5}$ during wet season was higher than the dry season. The highest OC and EC concentrations were observed in the transboundary haze period - with OC approximately 5 times higher and EC slightly higher than the background air. The higher OC and EC in particles indicated that they were caused by mixed aerosols, from both vehicles (diesel engines) and biomass burning, but dominated by biomass burning. This agrees with Andreae and Merlet (2001), who indicated that particles from biomass burning were generally dominated by carbonaceous components, from the thermal breakdown of cellulose, hemicellulose and lignin. Eight carbon fractions are widely used for source identification of the carbonaceous aerosols. The OC1 fraction in $PM_{2.5}$ mostly contains volatile organics, which can evaporate during long-range transport (Phairuang et al., 2020). OC2 is a good indicator for secondary organic carbon (SOC) formation, as well as biomass burning and motor vehicle exhaust (Chow et al., 2004). OC3 and EC1-PyC are the most abundant fractions of OC in biomass burning (Cao et al., 2005; Chuang et al., 2013; Pani et al., 2019). On the other hand, EC2 and EC3 represented motor vehicle emissions (Phairuang et al., 2020). OC2 and OC3 were the most abundant fractions, during the wet season as a result of transboundary haze. This indicated the significant contribution of biomass burning to carbonaceous aerosols (Chuang et al., 2013; Pani et al., 2019). This agrees with previous studies by Phairuang et al. (2020) and Dejchanchaiwong et al. (2020). The dominance of SOC during the transboundary haze period indicated more significant SOA formation (Lee et al., 2010). This agrees well with the increase of WSOC, which also suggests influence of SOA (Sullivan et al., 2006; Miyazaki et al., 2006). An increase of particulates from peat fires could provide organic precursors to react with the volatile organic compounds (VOCs) and form the SOA. It is noted that the EC tracer method has uncertainties, because the effects of emission from various sources and weather conditions cannot be assessed (Lee et al., 2010).

The OC/EC ratios during both wet and dry seasons suggested mixed sources - both vehicle combustion and biomass burning. However, the increment of OC/EC ratios in $PM_{2.5}$ in the present study during wet season can be explained by an increasing regional effect as no significant change of local sources occurred. The high OC/EC ratio during transboundary haze period also suggested that it was caused by mixed types of aerosol from both vehicle combustion and biomass burning emissions, but strongly dominated by biomass burning. Our ratios were similar to those measured by See et al. (2006), during a haze period in Singapore (2.78), Fujii et al. (2014) in Riau, Indonesia (2.99 $\pm$ 0.74), Fujii et al. (2016a) in Bangi, Malaysia (2.69 $\pm$ 0.93) and Tham et al. (2019) in Singapore (4.8 $\pm$ 2.5). The OC/EC ratios in ambient air during the

transboundary haze period were much lower than those reported near the source earlier by Fujii et al. (2014) in Riau (36.4 ± 9.08) and Tham et al. (2019) in Jambi, Provinces in Indonesia (20.4 ± 8.7). In the background air, the OC/EC ratio was 2.8 ± 0.4, similar to See et al. (2006) and Tham et al. (2019) in Singapore in normal periods - 1.94 and 2.3 ± 1.0, respectively. This agrees with the studies of PM emission sources in Hat Yai (Chomanee et al., 2020; Phairuang et al., 2020; Choochuay et al.,2020a, 2020b, 2020c). The OC, WSOC and OC/EC ratios were all much higher during the transboundary haze period in this study compared to seasonal averages, suggesting a higher pollution level of organic compounds and enhanced secondary formation during this period. Although the OC/EC ratio during the transboundary haze period was higher, the ratios of WSOC/OC were nearly unchanged (~0.4 in the transboundary haze and ~0.5 in the background). This is consistent with Budisulistiorini et al. (2018), who reported WSOC/OC = 0.6, during the 2015 haze event in Singapore.

The concentration of the biomass burning tracer, K, during wet season was 5 times higher than those during dry season. The K increase during the wet season is clear because the significant increase in a regional source (Pachon et al., 2013). There was a dominance of Na during transboundary haze period, accounting for 45.5% of total elements. This was consistent with previous studies by Samae et al. (2021), who reported that Na was also the main elemental component from burning of rice straw. In addition, a largest contribution of Ca (48%) in the background and during the dry season indicated urban road dust as a source, suggested by Dahari et al. (2019) and Jain et al. (2018), as well as biomass burning (Samae et al., 2021). A significant increase of SO_4^{2-}, NH_4^+ and NO_3^- during transboundary haze period could lead to formation of SIA. Sulong et al. (2017) reported the release of precursor gases, e.g. SO_2, NO_2 and NH_3, from biomass burning, causing the formation of secondary aerosols. Similar observations by Amil et al. (2016) added them as the main sources during the haze period in Petaling Jaya, Malaysia (SIA coupled with biomass burning); Shen et al. (2009), Khan et al. (2016) and Xu et al. (2012) also made similar suggestions.

It is interesting that Mount Sinabung in north Sumatra erupted on June 9–10, 2019 in the middle of our sampling, June 7–22, 2019 (Global Volcanism Program et al., 2019). Effects from the eruption on air quality to southern Thailand were assessed. The 72-h backward trajectory of air mass from June 9–12, 2019 was simulated and shown in Fig. S3. It was found to not influence the concentration of particulates recorded in southern Thailand. According to Global Volcanism Program et al. (2019), volcanic ash from the Sinabung eruption was found within 14 km of the mountain, especially toward the southeast. Due to the weak wind flow of the southwest monsoon in early June, the movement of volcanic particles to the northern area of Southeast Asia can be considered minimal. Nevertheless, results from satellite images indicated that the plume of SO_2 may influence areas such as southern Thailand and increase the concentration of SO_4^{2-} in particulates, as shown in the higher concentration of SO_4^{2-} recorded in $PM_{2.5}$ during this particular time and contribute to SIA formation.

Average total PAH concentrations during the wet season were ~2 times higher than the dry season. Also, average total PAHs and BaP-TEQ concentrations, during the transboundary haze period, were ~2 times higher than the background. This indicated that the higher total PAHs during the transboundary haze period were derived from biomass burning (Urbancok et al., 2017), agreeing with Sulong et al. (2019). It can be seen that transboundary haze from biomass open burning caused an increase of PAHs and BaP-TEQ concentrations in many cities in lower SEA, including southern Thailand. Human exposure to particle PAHs, during the haze periods, led to a higher cancer risk, similar to other studies in southern Thailand (Chomanee et al., 2020), Malaysia (Jamhari et al., 2014) and Singapore (Urbancok et al., 2017).

The CMB model was used to apportion sources in the Hat Yai during the study period. It identified peatland fire emissions as the main source of $PM_{2.5}$ during the wet season (Jun 2019 to May 2020) in Hat Yai, whereas, during the dry season (Feb to Apr, 2020), the local sources, e.g. vehicle diesel engine combustion and local biomass burning, predominated. Thus, the high $PM_{2.5}$ levels during the wet season can be attributed to increased contributions from regional biomass burning. It is confirmed that the increment of PM level during transboundary haze period in southern Thailand was a regional effect from biomass burning, originated in peatland forest in Sumatra, Indonesia. This finding was further confirmed by the backward trajectory simulation. However, air quality in Hat Yai city was directly influenced by not only transboundary haze caused by regional sources but also are in fact intensified by local emissions, i.e., diesel combustion and biomass burning i.e., rubber wood and rice straw burning as well as secondary aerosol formation, SOA and SIA, in other unidentified sources. Secondary aerosol formation was more pronounced during the transboundary haze period compared to the normal period. Industries in the southern part of Thailand are mainly agricultural, especially natural rubber trees and rubber wood is a major source of energy (Tekasakul et al., 2008; Dejchanchaiwong et al., 2016). Rubber wood residues are the main fuel in many industries, but they release environmental pollutants, especially PM and PAHs, (Chomanee et al., 2018). Also, during the 2019–2020 season, paddy fields in Songkhla Province, Thailand, occupied ~28,000 ha, or 22.6% of the southern region (Office of Agricultural Economics Thailand, 2019). Some of this area was burnt after harvesting to remove stubble and prepare the land for new crops, during both wet and dry seasons. Additionally, most vehicles in the area were diesel powered, due to fuel low price, and multi-purpose use of pick-up trucks.

5. Conclusion

The physical and chemical properties of $PM_{2.5}$ collected, in wet and dry seasons, in Hat Yai, were significantly different. Regional sources significantly increased $PM_{2.5}$ levels, during the 2019 wet season, influenced by the transboundary haze, which led to concentrations approximately 4 times higher than those in the background. The average OC and EC $PM_{2.5}$ concentrations, during the wet season were ~2 times higher than dry season ones, but the highest concentrations were observed in the transboundary haze period. The contribution of OC during the transboundary haze period was as high as 48.6%. The OC fraction in $PM_{2.5}$ was also attributed to biomass burning, because the OC3 and OC2 fractions were the most abundant, during the wet season as well as in the transboundary haze period. This was confirmed by high OC/EC ratios. The major trace elements were Ca, K and Na during the wet season and Ca, Mg and K during the dry season. The most abundant of trace element, during the transboundary haze periods, was K, accounting for 46.4% of the total trace elements. The highest concentrations of heavy metals were found in the transboundary haze period, but they did not exceed the National Ambient Air Quality Standards. Of the WSIs components, SO_4^{2-} dominated, contributing to 70.7% of the total WSI components during the strong haze period compared to the background air (56.3%). Although Mount Sinabung, near the path of air mass trajectory, erupted during the sampling period, $PM_{2.5}$ concentration in Hat Yai City was minimally affected. However, it may have slightly increased the SO_4^{2-} concentration in $PM_{2.5}$.

Also, BaP-TEQ concentrations in the wet season were 2 times as high as in the dry season, due to the contribution from the transboundary haze, which was twice the background. Results from the CMB model indicated that the main sources were a mixture of petroleum and biomass combustion. The CMB source apportionment indicated that the dominant sources of $PM_{2.5}$ during the wet season were peatland fire (45%) and diesel (14%). In contrast, during the dry season, diesel combustion (52%) and rubber wood burning (18%) were the major influences on $PM_{2.5}$ in Hat Yai. Moreover, the CMB model clearly showed the major source of $PM_{2.5}$ during the transboundary haze period was peatland fires (50%). This was confirmed the air mass backward trajectories which showed airmasses moving over peatland fires in Sumatra, identified from hotspots in satellite images. Not only the primary sources, but also weather conditions and secondary formation, could

also play an important role in $PM_{2.5}$ concentrations in ambient air. Significant increase of WSI: SO_4^{2-}, NH_4^+ and NO_3^- and carbonecous component: SOC, during transboundary haze period in southern Thailand, suggested source contributions from SIA and SOA formations, respectively.

We concluded that $PM_{2.5}$ in the ambient air of Hat Yai City, southern Thailand, was mainly affected by local anthropogenic sources, especially diesel combustion and local biomass burning, i.e. rubber wood and rice straw burnt during most of the year (background), but intensified from transboundary haze from peatland fires in Sumatra in the haze period in the wet season: this has been occurring nearly annually now, but intensified in the El Niño years.

CRediT authorship contribution statement

Preyapon Promsiri: Data curation, Formal analysis, Writing – original draft, Collected the data, Contributed data or analysis tools, Performed the analysis, Wrote the paper Draft a manuscript. **Surajit Tekasakul:** Formal analysis, Performed the analysis Discuss the results, Other contribution Advice the procedure and problem solving. **Thunyapat Thongyen:** Formal analysis, Other contribution Advice the procedure and problem solving for OC and EC analysis. **Panwadee Suwattiga:** Data curation, Collected the data, Other contribution Give advices and comments. **John Morris:** Writing – original draft, Writing – review & editing, Wrote the paper Edit manuscript, Other contribution Give advices and comments. **Mohd Talib Latif:** Writing – original draft, Wrote the paper. **Perapong Tekasakul:** Formal analysis, Writing – original draft, Writing – review & editing, Performed the analysis Discuss and conclude the results, Wrote the paper Edit manuscript, Other contribution, Project administration. **Racha Dejchanchaiwong:** Formal analysis, Writing – original draft, Writing – review & editing, Conceived and designed the analysis, Supervision, and Design of, Methodology, Performed the analysis Discuss and conclude the results, Wrote the paper, Write and edit manuscript, Other contribution, Funding acquisition.

Declaration of competing interest

The authors declare that they have no known competing financial interests or personal relationships that could have appeared to influence the work reported in this paper.

Data availability

Data will be made available on request.

Acknowledgments

This research was supported by National Science, Research and Innovation Fund (NSRF) and Prince of Songkla University (Grant No. ENG6505016M) and the Interdisciplinary Graduate School of Energy Systems, Prince of Songkla University under grant number 1-2018/07.

Appendix A. Supplementary data

Supplementary data to this article can be found online at https://doi.org/10.1016/j.atmosenv.2022.119512.

References

Adam, M.G., Tran, P.T.M., Bolan, N., Balasubramanian, R., 2020. Biomass burning-derived airborne particulate matter in Southeast Asia: a critical review. J. Hazard Mater. 124760. https://doi:10.1016/j.jhazmat.2020.124760.

Air Resources Laboratory, 2021. HYSPLIT model. Available: https://ready.arl.noaa.gov/hypub-bin/trajtype.pl?runtype=archive. (Accessed 19 December 2020).

Amil, N., Latif, M.T., Khan, M.F., Mohamad, M., 2016. Seasonal variability of $PM_{2.5}$ composition and sources in the Klang Valley urban-industrial environment. Atmos. Chem. Phys. 16, 5357–5381. https://doi.org/10.5194/acp-16-5357-2016.

Andreae, M.O., Merlet, P., 2001. Emission of trace gases and aerosols from biomass burning. Global Biogiochemical Cycles 15 (4), 955–966. https://doi.org/10.5194/acp-19-8523-2019.

Apte, J.S., Brauer, M., Cohen, A.J., Ezzati, M., Pope, C.A., 2018. Ambient $PM_{2.5}$ reduces global and regional life expectancy. Environ. Sci. Technol. Lett. 5, 546–551. https://doi:10.1021/acs.estlett.8b00360.

ASMC, 2021. Southeast Asia's air quality and haze situation report. Available: http://asmc.asean.org. (Accessed 4 January 2021).

Betha, R., Behera, S.N., Balasubramanian, R., 2014. Southeast Asian smoke haze: fractionation of particulate-bound elements and associated health risk. Environ. Sci. Technol. 48 (8), 4327–4335. https://doi:10.1021/es405533d.

Betha, R., Pradani, M., Lestari, P., Joshi, U.M., Reid, J.S., Balasubramanian, R., 2013. Chemical speciation of trace metals emitted from Indonesian peat fires for health risk assessment. Atmos. Res. 122, 571–578. https://doi:10.1016/j.atmosres.2012.05.024.

Budisulistiorini, S.H., Riva, M., Williams, M., Miyakawa, T., Chen, J., Itoh, M., et al., 2018. Dominant contribution of oxygenated organic aerosol to haze particles from real-time observation in Singapore during an Indonesian wildfire event in 2015. Atmos. Chem. Phys. 18 (22), 16481–16498. https://doi:10.5194/acp-18-16481-2018.

Cao, J.J., Wu, F., Chow, J.C., Lee, S.C., Li, Y., Chen, S.W., et al., 2005. Characterization and source apportionment of atmospheric organic and elemental carbon during fall and winter of 2003 in Xi'an, China. Atmos. Chem. Phys. 5 (11), 3127–3137. https://doi:10.5194/acp-5-3127-2005.

Chen, Q., Taylor, D., 2018. Transboundary atmospheric pollution in Southeast Asia: current methods, limitations and future developments. Crit. Rev. Environ. Sci. Technol. 1–33. https://doi:10.1080/10643389.2018.1493337.

Chomanee, J., Tekasakul, S., Tekasakul, P., Furuuchi, M., 2018. Effect of irradiation energy and residence time on decomposition efficiency of polycyclic aromatic hydrocarbons (PAHs) from rubber wood combustion emission using soft X-rays. Chemosphere 210, 417–423. https://doi:10.1016/j.chemosphere.2018.07.001.

Chomanee, J., Thongboon, K., Tekasakul, S., Furuuchi, M., Dejchanchaiwong, R., Tekasakul, P., 2020. Physicochemical and toxicological characteristics of nanoparticles in aerosols in southern Thailand during recent haze episodes in lower Southeast Asia. J. Environ. Sci. 94, 72–80. https://doi:10.1016/j.jes.2020.03.021.

ChooChuay, C., Pongpiachan, S., Tipmanee, D., Deelaman, W., Iadtem, N., Suttinun, O., et al., 2020b. Effects of Agricultural Waste Burning on $PM_{2.5}$-Bound Polycyclic Aromatic Hydrocarbons, Carbonaceous Compositions, and Water-Soluble Ionic Species in the Ambient Air of Chiang-Mai, Thailand, vols. 1–22. Polycyclic Aromatic Compounds. https://doi:10.1080/10406638.2020.1750436.

ChooChuay, C., Pongpiachan, S., Tipmanee, D., Deelaman, W., Suttinun, O., Wang, Q., et al., 2020a. Long-range transboundary atmospheric transport of polycyclic aromatic hydrocarbons, carbonaceous compositions, and water-soluble ionic species in southern Thailand. Aerosol Air Qual. Res. 20, 1591–1606. https://doi:10.4209/aaqr.2020.03.0120.

ChooChuay, C., Pongpiachan, S., Tipmanee, D., Suttinun, O., Deelaman, W., Wang, Q., et al., 2020c. Impacts of $PM_{2.5}$ sources on variations in particulate chemical compounds in ambient air of Bangkok, Thailand. Atmos. Pollut. Res. 11, 1657–1667. https://doi:10.1016/j.apr.2020.06.030.

Chow, J.C., Watson, J.G., Chen, L.-W.A., Arnott, W.P., Moosmüller, H., Fung, K., 2004. Equivalence of elemental carbon by thermal/optical reflectance and transmittance with different temperature protocols. Environ. Sci. Technol. 38 (16), 4414–4422. https://doi:10.1021/es034936u.

Chu, S.-H., 2005. Stable estimate of primary OC/EC ratios in the EC tracer method. Atmos. Environ. 39 (8), 1383–1392. https://doi:10.1016/j.atmosenv.2004.11.038.

Chuang, M.-T., Chou, C.C.-K., Sopajaree, K., Lin, N.-H., Wang, J.-L., Sheu, G.-R., et al., 2013. Characterization of aerosol chemical properties from near-source biomass burning in the northern Indochina during 7-SEAS/Dongsha experiment. Atmos. Environ. 78, 72–81. https://doi:10.1016/j.atmosenv.2012.06.056.

Dahari, N., Muda, K., Latif, M.T., Hussein, N., 2019. Studies of atmospheric $PM_{2.5}$ and its inorganic water soluble ions and trace elements around Southeast Asia: a review. Asia-Pacific Journal of Atmospheric Sciences 57, 361–385. https://doi:10.1007/s13143-019-00132-x.

Dallmann, T.R., Onasch, T.B., Kirchstetter, T.W., Worton, D.R., Fortner, E.C., Herndon, S.C., et al., 2014. Characterization of particulate matter emissions from on-road gasoline and diesel vehicles using a soot particle aerosol mass spectrometer. Atmos. Chem. Phys. 14, 7585–7599. https://doi.org/10.5194/acp-14-7585-2014, 2014.

Dejchanchaiwong, R., Kumar, A., Tekasakul, P., 2016. Performance and economic analysis of natural convection based rubber smoking room for rubber cooperatives in Thailand. Renew. Energy 132, 233–242. https://doi.org/10.1016/j.renene.2018.07.145.

Dejchanchaiwong, R., Tekasakul, P., 2021. Effects of coronavirus induced city lockdown on $PM_{2.5}$ and gaseous pollutant concentrations in Bangkok. Aerosol Air Qual. Res. 21, 200418 https://doi.org/10.4209/aaqr.200418.

Dejchanchaiwong, R., Tekasakul, P., Tekasakul, S., Phairuang, W., Nim, N., Sresawasd, C., et al., 2020. Impact of transport of fine and ultrafine particles from open biomass burning on air quality during 2019 Bangkok haze episode. J. Environ. Sci. 97, 149–161. https://doi:10.1016/j.jes.2020.04.009.

Earthdata, 2021. NRT VIIRS 375 m active fire product VNP14IMGT. Available: https://earthdata.nasa.gov/firms. (Accessed 4 January 2021).

EEA, 2008. Air quality, air quality standards with directive 2008/50/EU. Available. https://ec.europa.eu/environment/air/quality/standards.htm. prepared by European Environment Agency. (Accessed 5 September 2021). European Union.

Engling, G., He, J., Betha, R., Balasubramanian, R., 2014. Assessing the regional impact of Indonesian biomass burning emissions based on organic molecular tracers and chemical mass balance modeling. Atmos. Chem. Phys. 14, 8043–8054. https://doi.org/10.5194/acp-14-8043-2014.

Feng, X., Wei, S., Wang, S., 2020. Temperature inversions in the atmospheric boundary layer and lower troposphere over the Sichuan Basin, China: climatology and impacts on air pollution. Sci. Total Environ. 726, 138579 https://doi.org/10.1016/j.scitotenv.2020.138579.

Fujii, Y., Huboyo, H.S., Tohno, S., Okuda, T., Syafrudin, 2019. Chemical speciation of water-soluble ionic components in $PM_{2.5}$ derived from peatland fires in Sumatra Island. Atmos. Pollut. Res. 10, 1260–1266. https://doi:10.1016/j.apr.2019.02.009.

Fujii, Y., Iriana, W., Oda, M., Puriwigati, A., Tohno, S., Lestari, P., et al., 2014. Characteristics of carbonaceous aerosols emitted from peatland fire in Riau, Sumatra, Indonesia. Atmos. Environ. 87, 164–169. https://doi:10.1016/j.atmosenv.2014.01.037.

Fujii, Y., Mahmud, M., Oda, M., Tohno, S., Matsumoto, J., Mizohata, A., 2016b. A Key indicator of transboundary particulate matter pollution derived from Indonesian peatland fires in Malaysia. Aerosol Air Qual. Res. 16, 69–78. https://doi.org/10.4209/aaqr.2015.04.0215.

Fujii, Y., Mahmud, M., Tohno, S., Okuda, T., Mizohata, A., 2016a. A case study of $PM_{2.5}$ characterization in Bangi, Selangor, Malaysia during the southwest monsoon season. Aerosol Air Qual. Res. 16, 2685–2691. https://doi.org/10.4209/aaqr.2015.04.0277.

Fujii, Y., Tohno, S., Amil, N., Latif, M.T., 2017. Quantitative assessment of source contributions to PM 2.5 on the west coast of Peninsular Malaysia to determine the burden of Indonesian peatland fire. Atmos. Environ. 171, 111–117. https://doi:10.1016/j.atmosenv. 2017.10.009.

Fujii, Y., Tohno, S., Amil, N., Latif, M.T., Oda, M., Matsumoto, J., Mizohata, A., 2015. Annual variations of carbonaceous $PM2.5$ in Malaysia: influence by Indonesian peatland fires. Atmos. Chem. Phys. 15 (23), 13319–13329. https://doi:10.5194/acp-15-13319-2015.

Furuuchi, M., Murase, T., Tsukawaki, S., Hang, P., Sieng, S., Hata, M., 2007. Characteristics of ambient particle-bound polycyclic aromatic hydrocarbons in the Angkor monument area of Cambodia. Aerosol Air Qual. Res. 7, 221–238. https://doi.org/10.4209/aaqr.2007.01.0001.

Global Volcanism Program, 2019. Report on Sinabung (Indonesia). In: Crafford, A.E., Venzke, E. (Eds.), Bulletin of the Global Volcanism Network, vol. 44. Smithsonian Institution, p. 8. https://doi.org/10.5479/si.GVP.BGVN201908-261080.

Ho, A.F.W., Zheng, H., Earnest, A., Cheong, K.H., Pek, P.P., Seok, J.Y., et al., 2019. Time-stratified case crossover study of the association of outdoor ambient air pollution with the risk of acute myocardial infarction in the context of seasonal exposure to the Southeast Asian haze problem. J. Am. Heart Assoc. 8 (6), e011272. https://doi:10.1161/jaha.118.011272.

Intra, P., Yawootti, A., Tippayawong, N., 2013. An electrostatic sensor for the continuous monitoring of particulate air pollution. Kor. J. Chem. Eng. 30 (12), 2205–2212. https://doi:10.1007/s11814-013-0168-7.

Jaafar, S.A., Latif, M.T., Razak, I.S., Wahid, N.B.A., Khan, M.F., Srithawirat, T., 2018. Composition of carbohydrates, surfactants, major elements and anions in $PM_{2.5}$ during the 2013 Southeast Asia high pollution episode in Malaysia. Particuology 37, 119–126. https://doi:10.1016/j.partic.2017.04.012.

Jain, S., Sharma, S.K., Mandal, T.K., Saxena, M., 2018. Source apportionment of PM 10 in Delhi, India using PCA/APCS, UNMIX and PMF. Particuology 37, 107–118. https://doi:10.1016/j.partic.2017.05.009.

Jamhari, A.A., Sahani, M., Latif, M.T., Chan, K.M., Tan, H.S., Khan, M.F., Mohd Tahir, N., 2014. Concentration and source identification of polycyclic aromatic hydrocarbons (PAHs) in PM10 of urban, industrial and semi-urban areas in Malaysia. Atmos. Environ. 86, 16–27. https://doi:10.1016/j.atmosenv.2013.12.019.

Khan, M.F., Latif, M.T., Amil, N., Juneng, L., Mohamad, N., Nadzir, M.S.M., et al., 2015. Characterization and source apportionment of particle number concentration at a semi-urban tropical environment. Environ. Sci. Pollut. Control Ser. 22 (17), 13111–13126. https://doi:10.1007/s11356-015-4541-4.

Khan, M.F., Latif, M.T., Saw, W.H., Amil, N., Nadzir, M.S.M., Sahani, M., et al., 2016. Fine particulate matter in the tropical environment: monsoonal effects, source apportionment, and health risk assessment. Atmos. Chem. Phys. 16, 597–617. https://doi.org/10.5194/acp-16-597-2016, 2016.

Kumsanlas, N., Piriyakarnsakul, S., Sok, P., Hongtieab, S., Ikemori, F., Szymanski, W.W., Hata, M., Otani, Y., Furuuchi, M., 2019. A cascade air sampler with multi-nozzle inertial filters for $PM0_{.1}$. Aerosol Air Qual. Res. 19, 1666–1677. https://doi.org/10.4209/aaqr.2019.02.0066.

Latif, M.T., Othman, M., Idris, N., Juneng, L., Abdullah, A.M., Hamzah, W.P., Jaafar, A. B., 2018. Impact of regional haze towards air quality in Malaysia: a review. Atmos. Environ. 177, 28–44. https://doi:10.1016/j.atmosenv.2018.01.002.

Lee, S., Wang, Y., Rusell, A.G., 2010. Assessment of secondary organic carbon in the southeastern United States: a review. J. Air Waste Manag. Assoc. 60 (11), 1282–1292. https://doi:10.3155/1047-3289.60.11.1282.

Ling, C.H., Ahmed, K., Binti Muhamad, R., Shahbaz, M., 2015. Decomposing the trade-environment nexus for Malaysia: what do the technique, scale, composition, and comparative advantage effect indicate? Environ. Sci. Pollut. Control Ser. 22 (24), 20131–20142. https://doi:10.1007/s11356-015-5217-9.

Lippmann, M., Thurston, G.D., 1996. Sulfate concentrations as an indicator of ambient particulate matter air pollution for health risk evaluations. J. Expo. Anal. Environ. Epidemiol. 1996, 123–146. PMID: 8792293.

Mahasakpan, N., Chaisongkaew, P., Inerb, M., Nim, N., Phairuang, W., Tekasakul, S., Furuuchi, M., Hata, M., Kaosol, T., Tekasakul, P., Dejchanchaiwong, R., 2023. Fine and ultrafine particle- and gas-polycyclic aromatic hydrocarbons affecting southern Thailand air quality during transboundary haze and potential health effects. J. Environ. Sci. 124, 253–267. https://doi.org/10.1016/j.jes.2021.11.005.

Miyazaki, Y., Kondo, Y., Takegawa, N., Komazaki, Y., Kawamura, K., Mochida, M., Okuzawa, K., Weber, R.J., 2006. Time-resolved measurements of water-soluble organic carbon in Tokyo. J. Geophys. Res. 111, D23206. https://doi:10.1029/2006JD007125.

Na, K., Sawant, A.A., Song, C., Cocker, D.R., 2004. Primary and secondary carbonaceous species in the atmosphere of Western Riverside County, California. Atmos. Environ. 38, 1345–1355. https://doi.org/10.1016/j.atmosenv.2003.11.023.

Office of Agricultural Economics Thailand, 2019. Centre for Agricultural Information. https://www.oae.go.th/assets/portals/1/files/socio/LandUtilization2562.pdf. (Accessed 29 July 2021).

Othman, J., Sahani, M., Mahmud, M., Sheikh Ahmad, M.K., 2014. Transboundary smoke haze pollution in Malaysia: inpatient health impacts and economic valuation. Environ. Pollut. 189, 194–201. https://doi:10.1016/j.envpol.2014.03.010.

Ouyang, W., Guo, B., Cai, G., Li, Q., Han, S., Liu, B., Liu, X., 2015. The washing effect of precipitation on particulate matter and the pollution dynamics of rainwater in downtown Beijing. Sci. Total Environ. 505, 306–314. https://doi.org/10.1016/j.scitotenv.2014.09.062.

Pachon, J.E., Weber, R.J., Zhang, X., Mulholland, J.A., Russell, A.G., 2013. Revising the use of potassium (K) in the source apportionment of PM2.5. Atmos. Pollut. Res. 4, 14–21. https://doi.org/10.5094/APR.2013.002.

Pani, S.K., Chantara, S., Khamkaew, C., Lee, C.-T., Lin, N.-H., 2019. Biomass burning in the northern peninsular Southeast Asia: aerosol chemical profile and potential exposure. Atmos. Res. 224, 180–195. https://doi:10.1016/j.atmosres.2019.03.031.

PCD, 2021. Air quality standards in the atmosphere in Thailand. http://air4thai.pcd.go.th/webV2/download.php?grpIndex=1. (Accessed 18 September 2021).

Phairuang, W., Inerb, M., Furuuchi, M., Hata, M., Tekasakul, S., Tekasakul, P., 2020. Size-fractionated carbonaceous aerosols down to PM0.1 in southern Thailand: local and long-range transport effects. Environ. Pollut. 260, 114031. https://doi:10.1016/j.envpol.2020.114031.

Rajput, P., Izhar, S., Gupta, T., 2018. Deposition modeling of ambient aerosols in human respiratory system: health implication of fine particles penetration into pulmonary region. Atmos. Pollut. Res. 10 (1), 334–343. https://doi:10.1016/j.apr.2018.08.013.

Ram, K., Sarin, M.M., Tripathi, S.N., 2012. Temporal trends in atmospheric PM2.5, PM10, elemental carbon, organic carbon, water-soluble organic carbon, and optical properties: impact of biomass burning emissions in the Indo-Gangetic Plain. Environ. Sci. Technol. 46, 686–695. https://doi:10.1021/es202857w.

Ram, K., Sarin, M.M., Hegde, P., 2008. Atmospheric abundances of primary and secondary carbonaceous species at two high-altitude sites in India: sources and temporal variability. Atmos. Environ. 42 (28), 6785–6796. https://doi:10.1016/j.atmosenv. 2008.05.031.

Ramakreshnan, L., Aghamohammadi, N., Fong, C.S., Bulgiba, A., Zaki, R.A., Wong, L.P., Sulaiman, N.M., 2017. Haze and health impacts in ASEAN countries: a systematic review. Environ. Sci. Pollut. Control Ser. 25 (3), 2096–2111. https://doi:10.1007/s11356-017-0860-y.

Samae, H., Tekasakul, S., Tekasakul, P., Furuuchi, M., 2021. Emission factors of ultrafine particulate matter ($PM<0.1$ μm) and particle-bound polycyclic aromatic hydrocarbons from biomass combustion for source apportionment. Chemosphere 262, 127846. https://doi:10.1016/j.chemosphere.2020.127846.

Samsuddin, N.A.C., Khan, M.F., Maulud, K.N.A., Hamid, A.H., Munna, F.T., Rahim, M.A. A., et al., 2018. Local and transboundary factors' impacts on trace gases and aerosol during haze episode in 2015 El Niño in Malaysia. Sci. Total Environ. 630, 1502–1514. https://doi:10.1016/j.scitotenv.2018.02.289.

See, S.W., Balasubramanian, R., Rianawati, E., Karthikeyan, S., Streets, D.G., 2007. Characterization and source apportionment of particulate matter $\leq$ 2.5 μm in Sumatra, Indonesia, during a recent peat fire episode. Environ. Sci. Technol. 41 (10), 3488–3494. https://doi:10.1021/es061943k.

See, S.W., Balasubramanian, R., Wang, W., 2006. A study of the physical, chemical, and optical properties of ambient aerosol particles in Southeast Asia during hazy and nonhazy days. J. Geophys. Res. Atmos. 111 (D10S08). https://doi:10.1029/2005jd006180.

Shen, Z., Cao, J., Tong, Z., Liu, S., Reddy, L.S.S., Han, Y., et al., 2009. Chemical characteristics of submicron particles in winter in Xi'an. Aerosol Air Qual. Res. 9, 80–93. https://doi.org/10.4209/aaqr.2008.10.0050.

Sresawasd, C., Chetiyanukornkul, T., Suriyawong, P., Tekasakul, S., Furuuchi, M., Hata, M., Malinee, R., Tekasakul, P., Dejchanchaiwong, R., 2021. Influence of meteorological conditions and fire hotspots on $PM_{0.1}$ in northern Thailand during strong haze episodes and carbonaceous aerosol characterization. Aerosol Air Qual. Res. 21 (11), 210069 https://doi.org/10.4209/aaqr.210069.

Sudheer, A.K., Sarin, M.M., 2008. Carbonaceous aerosols in MABL of Bay of Bengal: influence of continental outflow. Atmos. Environ. 42 (18), 4089–4100. https://doi:10.1016/j.atmosenv.2008.01.033.

Sullivan, A.P., Peltier, R.E., Brock, C.A., de Gouw, J.A., Holloway, J.S., Warneke, C., Wollny, A.G., Weber, R.J., 2006. Airborne measurements of carbonaceous aerosol soluble in water over northeastern United States: method development and an investigation into water-soluble organic carbon sources. J. Geophys. Res. 111, D23S46. https://doi:10.1029/2006JD007072.

Sulong, N.A., Latif, M.T., Khan, M.F., Amil, N., Ashfold, M.J., Wahab, M.I.A., et al., 2017. Source Apportionment and Health Risk Assessment Among Specific Age Groups during Haze and Non-haze Episodes in Kuala Lumpur, Malaysia, vols. 601–602. Science of The Total Environment, pp. 556–570. https://doi:10.1016/j.scitotenv.2017.05.153.

Sulong, N.A., Latif, M.T., Sahani, M., Khan, M.F., Fadzil, M.F., Tahir, N.M., et al., 2019. Distribution, sources and potential health risks of polycyclic aromatic hydrocarbons (PAHs) in $PM_{2.5}$ collected during different monsoon seasons and haze episode in Kuala Lumpur. Chemosphere 219, 1–14. https://doi:10.1016/j.chemosphere.2018.11.195.

Tahir, N.M., Koh, M., Suratman, S., 2013b. $PM_{2.5}$ and associated ionic species in a sub-urban coastal area of Kuala Terengganu, southern south China sea (Malaysia). Sains Malays. 42 (8), 1065–1072.

Tahir, N.M., Suratman, S., Fong, F.T., Hamzah, M.S., Latif, M.T., 2013a. Temporal distribution and chemical characterization of atmospheric particulate matter in the Eastern coast of peninsular Malaysia. Aerosol Air Qual. Res. 13, 584–595. https://doi.org/10.4209/aaqr.2012.08.0216.

Tang, N., Hattori, T., Taga, R., Igarashi, K., Yang, X., Tamura, K., et al., 2005. Polycyclic aromatic hydrocarbons and nitropolycyclic aromatic hydrocarbons in urban air particulates and their relationship to emission sources in the Pan-Japan Sea Countries. Atmos. Environ. 39, 5817–5826. https://doi.org/10.1016/j.atmosenv.2005.06.018.

Tang, X., Zhang, X.S., Wang, Z.W., Ci, Z.J., 2016. Water-soluble organic carbon (WSOC) and its temperature-resolved carbon fractions in atmospheric aerosols in Beijing. Atmos. Res. 181, 200–210. https://doi:10.1016/j.atmosres.2016.06.019.

Tekasakul, P., Furuuchi, M., Tekasakul, S., Chomanee, J., Otani, Y., 2008. Characteristics of PAHs in particulates in the atmospheric environment of Hat Yai City, Thailand, and relationship with rubber-wood burning in rubber sheet production. Aerosol Air Qual. Res. 8 (3), 265–278. https://doi:10.4209/aaqr.2008.02.0004.

Tham, J., Sarkar, S., Jia, S., Reid, J.S., Mishra, S., Sudiana, I.M., et al., 2019. Impacts of peat-forest smoke on urban $PM_{2.5}$ in the Maritime Continent during 2012–2015: carbonaceous profiles and indicators. Environ. Pollut. 248, 496–505. https://doi:10.1016/j.envpol.2019.02.049.

Thongyen, T., Hata, M., Toriba, A., Ikeda, T., Koyama, H., Otani, Y., Furuuchi, M., 2015. Development of $PM_{0.1}$ personal sampler for evaluation of personal exposure to aerosol nanoparticles. Aerosol Air Qual. Res. 15, 180–187. https://doi.org/10.4209/aaqr. 2014.05.0102.

TMD, 2021. Climate data. Available: http://www.aws-observation.tmd.go.th/web/climate/climate_past.asp. (Accessed 29 June 2021).

U.S.EPA, 2004a. Protocol for Applying and Validating the CMB Model for PM2.5 and VOC. .S. Environmental Protection Agency, Research Triangle Park, NC. Report No. EPA-451/R-04-001 prepared by U.

U.S.EPA, 2004b. EPA-CMB8.2 User's Manual. Report No. EPA-452/R-04-011 Prepared by U.S. Environmental Protection Agency, Research Triangle Park, NC.

U.S.EPA, 2005. EPA-CMB8.2 model code. Available. https://www.epa.gov/scram/chemical-mass-balance-cmb-model. (Accessed 20 August 2021).

U.S.EPA, 2016. Sampling Points for Air Quality, Representativeness and Comparability of Measurement in Accordance with Directive 2008/50/EC on Ambient Air Quality and Cleaner Air for Europe. Policy Department for Economic, Scientific and Quality of Life Policies. Available:https://www.europarl.europa.eu/RegData/etudes/STUD/2019/631055/IPOL_STU(2019)631055_EN.pdf. (Accessed 20 July 2021).

Uda, S.K., Hein, L., Atmoko, D., 2019. Assessing the health impacts of peatland fires: a case study for Central Kalimantan, Indonesia. Environ. Sci. Pollut. Control Ser. 26, 31315–31327. https://doi.org/10.1007/s11356-019-06264-x.

Urbancok, D., Payne, A.J.R., Webster, R.D., 2017. Regional transport, source apportionment and health impact of PM 10 bound polycyclic aromatic hydrocarbons in Singapore's atmosphere. Environ. Pollut. 229, 984–993. https://doi:10.1016/j.envpol.2017.07.086.

Xu, J.Q., Chen, L.Y., Choi, H., Li, X.C., 2012. Theoretical study and pathways for nanoparticle capture during solidification of metal melt. J. Phys. Condens. Matter 24 (25), 255304. https://doi:10.1088/0953-8984/24/25/255304.

Xu, J., Tai, X., Betha, R., He, J., Balasubramanian, R., 2014. Comparison of physical and chemical properties of ambient aerosols during the 2009 haze and non-haze periods in Southeast Asia. Environ. Geochem. Health 37 (5), 831–841. https://doi:10.1007/s10653-014-9667-7.

Zhang, Y.X., Shao, M., Zhang, Y.H., Zeng, L.M., He, L.Y., Zhu, B., 2007. Source profiles of particulate organic matters emitted from cereal straw burnings. J. Environ. Sci. 19 (2), 167–175. https://doi.org/10.1016/S1001-0742(07)60027-8.

Zhang, Z.H., Khlystov, A., Norford, L.K., Tan, Z.K., Balasubramanian, R., 2017. Characterization of traffic-related ambient fine particulate matter (PM2.5) in an Asian city: environmental and health implications. Atmos. Environ. 161, 132–143. https://doi.org/10.1016/j.atmosenv.2017.04.040.